ECCOMAS Congress 2016
VII European Congress on Computational Methods in Applied Sciences and Engineering
M. Papadrakakis, V. Papadopoulos, G. Stefanou, V. Plevris (eds.)
Crete Island, Greece, 5–10 June 2016

# CONSISTENT NON-REFLECTING BOUNDARY CONDITIONS FOR BOTH STEADY AND UNSTEADY FLOW SIMULATIONS IN TURBOMACHINERY APPLICATIONS

**Daniel Schlüß, Christian Frey, Graham Ashcroft**

German Aerospace Center (DLR)
Institute of Propulsion Technology
Linder Höhe, 51147 Cologne, Germany
email: daniel.schluess@dlr.de, christian.frey@dlr.de, graham.ashcroft@dlr.de

**Keywords:** Non-Reflecting Boundary Conditions, Turbomachinery, Steady and Unsteady CFD

**Abstract.** *This paper presents the implementation of a non-reflecting boundary condition for steady and unsteady turbomachinery flow computations. Here, the truncation of the computational domain can lead to spurious numerical reflections due to artificial open boundary surfaces. To face this issue, Giles introduces a popular set of non-reflecting boundary conditions for turbomachinery applications. Whereas the steady formulation is exact within the linearisation approach, Giles suggests an approximate boundary condition for unsteady simulations. Resulting from this approximation, the unsteady boundary conditions are not perfectly non-reflecting. Thus, steady and time averaged unsteady flow solutions do not necessarily coincide, even if the flow field contains no unsteadiness.*

*We suggest a single boundary condition formulation suitable for steady and unsteady simulations. This approach applies a modal decomposition and, thus, undesired incoming modes can easily be ruled out. Steady modes can be handled as in the steady case. Apart from the assumptions made by starting from the linearised, two-dimensional Euler equations, this approach does not require any further approximation, and, therefore, the time-averaged unsteady and the steady solutions coincide in the limit of steady flows.*

*We apply and assess the presented boundary condition in steady and unsteady computations of two turbomachinery test cases.*

## 1 INTRODUCTION

Computational fluid dynamics (CFD) based upon the Reynolds-averaged Navier-Stokes equations (RANS) has become a vital tool for both design of and research on turbomachinery applications in the aerospace, energy and automotive industries. Steady computations remain the backbone of industrial design processes especially due to their extensive utilization in shape optimization methods. Unsteady turbomachinery flow simulations, on the other hand, attain increasing importance for understanding blade row interactions which is needed to achieve higher aerodynamic loads and closer blade row spacings to meet the desire for more efficient and lighter engines. Moreover, these design trends require additional activities in fluid dynamics related disciplines like aeroelasticity and aeroacoustics, which again heavily rely on unsteady CFD [1, 2].

The quality of flow simulations depends, beside the choice of an appropriate closure model for the RANS equations and the properties of the numerical scheme, directly on the boundary conditions imposed. Straightforward far-field or simple 1D characteristic boundary conditions can lead to spurious, numerical reflections deteriorating the flow solution inside. Thus, many aerodynamic problems, such as the flow around an airfoil or wing, are commonly simulated in very large computational domains to minimise the impact of the far-field boundary conditions on the region of interest.

In turbomachinery flows, however, this is usually not possible. Firstly, instead of the whole machine, only single components or certain sets of stages or blade rows are considered which leads to artificial, open boundaries rather close to the blades. Additionally in steady turbomachinery CFD, adjacent blade rows in their respective relative frames of reference are coupled via so-called mixing planes [3]. These mixing planes pose boundary conditions to the adjacent domains which strengthens the need for non-reflecting boundary conditions (NRBC) in turbomachinery applications.

Numerical reflections, that emerge when applying less advanced boundary conditions, can disturb the flow field in the neighbourhood of a blade leading to an incorrect surface pressure distribution and hence aerodynamic work or losses. We will give an example for this later in the application section. In particular, reflecting boundary conditions can deteriorate the prediction of aeroelastic or aeroacoustic phenomena as shown by Kersken et al. [4] and Ashcroft and Schulz [5].

The mathematical theory of non-reflecting boundary conditions is presented in a review paper by Hidgon [6]. Based upon this theory, Giles introduces a set of NRBC for 2D turbomachinery flows [7, 8]. Giles' approach assumes wavelike perturbations around an average flow state. Thus, the linearised Euler equations are considered neglecting viscous effects. Transforming these perturbations into the spectral, i.e. time and wavenumber, domain and exploiting an eigenvector analysis, one obtains a set of modal perturbations and their respective direction of propagation. This decomposition enables the definition of a flow state at the boundaries that does not induce undesired incoming perturbations. The straightforward implementation of these NRBC requires the frequencies and wave numbers of all perturbations at the boundary to be known. Due to the Fourier transform applied here, these boundary conditions are non-local in time and space. Therefore, Giles suggests an approximate boundary condition for unsteady computations derived from theoretical work of Engquist and Majda [9]. This boundary condition is derived from a Taylor series expansion about the ideal one-dimensional boundary condition and, thus, is local in time and space apart from the fact that it requires averaged quantities. A more detailed description of the implementation of these boundary conditions is given

in [10]. Saxer and Giles present an extension of the non-local, steady NRBC to 3D flows [11].

However, resulting from the approximation, Giles states the unsteady boundary conditions may produce significant unphysical reflections for outgoing modes with large circumferential wavenumbers [8]. Accordingly, steady solutions obtained utilizing the exact steady NRBC and time averaged unsteady flow solutions may differ even for naturally steady flows. Hagstrom proposes a higher order approach for the approximation of unsteady NRBC [12]. This method is local in time but employs a Fourier transform in space. Henninger et al. [13] apply it to acoustic and aeroelastic turbomachinery test cases and demonstrate improved non-reflecting properties compared to Giles' boundary condition.

To overcome the inconsistency of steady and unsteady NRBC and ensure their comparability in steady and time-accurate turbomachinery flow simulations, the authors propose a boundary condition formulation suitable for both. This approach applies a modal decomposition in time and circumferential direction. Thus, the zeroth harmonic in time can be handled by a steady boundary condition. Disturbances of higher harmonics are treated independently. Accordingly, undesired incoming modes can easily be ruled out. Apart from the assumptions made by starting from the linearised, two-dimensional Euler equations, this approach does not require any further approximation, and, therefore, the time-averaged unsteady and the steady solution coincide in the limit of steady flows.

In this paper, we firstly outline the theory behind NRBC and the approximation made by Giles. Subsequently, we present the implementation of an exact method and apply it to steady and unsteady turbomachinery computations. In order to validate our implementation of this boundary condition in DLR's 3D RANS solver for internal and turbomachinery flows, TRACE, we give a comparison to characteristic and 2D non-reflecting steady boundary conditions and approximate unsteady 2D NRBC. Thereby, the favourable behaviour of the exact method is demonstrated.

## 2 NON-REFLECTING BOUNDARY CONDITIONS

Before presenting our implementation of an exact boundary condition, we want to give a brief overview of one way to construct non-reflecting boundary conditions in the context of turbomachinery CFD as they are implemented in TRACE. A more elaborate description including the mathematical derivation and well-posedness analysis is given in Giles' technical report [7] and implementation details can be found in his UNSFLO report [10].

### 2.1 General approach

For many turbomachinery flows we can assume that variations in pitchwise direction predominate variations in spanwise direction [11]. Thus, we can adapt Giles' originally two-dimensional formulation for three-dimensional flows as a reasonable approximation. Here, the original technique is applied in blade-to-blade planes, i.e. the coupling of planes of constant relative channel height is neglected.

Let $q = (\varrho, u, v, w, p)$ be the vector of primitive variables with density $\varrho$, pressure $p$ and velocity components $u$,$v$ and $w$ aligned such that $u$ is normal to the boundary but in flow direction whilst $v$ and $w$ point along the boundary in pitchwise and spanwise direction, respectively. For the construction of non-reflecting boundary conditions we further consider sufficiently small perturbations around a mean flow state. So we can linearised the three-dimensional Euler equa-

tions in primitive form neglecting changes in spanwise direction:

$$\frac{\partial q}{\partial t} + A\frac{\partial q}{\partial x} + B\frac{\partial q}{\partial y} = 0 \tag{1}$$

with

$$A = \begin{pmatrix} \overline{u} & \overline{\varrho} & 0 & 0 & 0 \\ 0 & \overline{u} & 0 & 0 & 1/\overline{\varrho} \\ 0 & 0 & \overline{u} & 0 & 0 \\ 0 & 0 & 0 & \overline{u} & 0 \\ 0 & \gamma\overline{p} & 0 & 0 & \overline{u} \end{pmatrix} \text{ and } B = \begin{pmatrix} \overline{v} & 0 & \overline{\varrho} & 0 & 0 \\ 0 & \overline{v} & 0 & 0 & 0 \\ 0 & 0 & \overline{v} & 0 & 1/\overline{\varrho} \\ 0 & 0 & 0 & \overline{v} & 0 \\ 0 & 0 & \gamma\overline{p} & 0 & \overline{v} \end{pmatrix} \tag{2}$$

Overlined variables denote mean flow conditions and $\gamma$ represents the ideal gas heat capacity ratio. In the following, we only consider wave-like perturbations of the form

$$q = \mathrm{Re}\left(\hat{q}\, e^{\mathrm{i}(kx+my-\omega t)}\right) \tag{3}$$

where $x$ is again normal to the boundary in flow direction and $y$ is aligned with the boundary in pitchwise direction. Note that the latter is the circumferential direction in rotational turbomachinery flows. Then $k$ and $m$ denote wave numbers along $x$ and $y$, respectively, with angular frequency $\omega$. Though this approach seems rather restrictive, we can in fact assemble any flow state by superposition of these fundamental perturbations within the linearised theory. Substituting (3) into equation (1), we obtain:

$$\left(-\omega I + kA + mB\right)\hat{q} = 0 \tag{4}$$

With nontrivial solution $\hat{q}$, this yields the dispersion relation

$$\det\left(-\omega I + kA + mB\right) = 0 \tag{5}$$

or rearranged

$$\det\left(-\omega A^{-1} + kI + mA^{-1}B\right) = 0. \tag{6}$$

Assuming we know $\omega$ and $m$, equation (6) can be interpreted as a characteristic polynomial to the eigenvalue problem

$$\left(-\omega A^{-1} + mA^{-1}B\right) r = -kr \tag{7}$$

with eigenvalues $-k$ and right eigenvectors $r$. The 3D linearised Euler equations yield a characteristic polynomial of degree five. Accordingly, there are five eigenvalues $-k_i$ regarding their possible multiplicity. Analogously, we introduce a set of left eigenvectors $l_i$ satisfying

$$l_i\left(-\omega A^{-1} + mA^{-1}B\right) = -k_i l_i. \tag{8}$$

Note that the left eigenvectors are row vectors whereas the right eigenvectors are column vectors.

In order to derive non-reflecting boundary conditions from these mathematical considerations, it is helpful to clarify the physical interpretation of the left and right eigenvectors. As mentioned earlier, we can decompose any solution $q$ into a sum of single Fourier modes $\hat{q}$, each with distinct values of $\omega$ and $m$. Each of these modes is again a set of five fundamental waves with same $\omega$ and $m$ but (possibly) different $k$. Since the wave numbers normal to the boundary, $k_i$, are the negative eigenvalues of $(-\omega A^{-1} + mA^{-1}B)$, they allow us to distinguish whether the corresponding waves propagate into or out of the computational domain.

The change in primitive variables induced by such a wave is expressed by the respective right eigenvector $r_i$. In other words, the right eigenvectors form a set of linearly independent basis vectors and every perturbation from a mean state can be decomposed into a linear combination of right eigenvectors with weights $\alpha_i$ :

$$q = \mathrm{Re}\left(\left[\sum_{i=1}^{5} \alpha_i r_i e^{\mathrm{i}k_i x}\right] e^{\mathrm{i}(my-\omega t)}\right) \tag{9}$$

For different eigenvalues $k_i \neq k_j$, each left eigenvector $l_i$ is orthogonal to $r_j$, i.e. $l_i r_j = 0$. For eigenvalues of multiplicity larger than one, the corresponding eigenvectors can be constructed such that $l_i r_j = 0$ for $i \neq j$. Because of this perpendicularity relation, the left eigenvectors help us to determine the share of their corresponding right eigenvector in any arbitrary perturbation, i.e. $\alpha_i = l_i \hat{q}$. So the pivotal idea for the construction of non-reflecting boundary conditions is to decompose the flow state at a boundary and rule out the incoming waves. This can be done by requiring for any combination of $\omega$ and $m$

$$l_i \hat{q} = 0 \tag{10}$$

for each $l_i$ belonging to an incoming wave .

Applying the above to the three-dimensional linearised Euler equations, we obtain the following wave numbers:

$$k_{1,2,3} = \frac{\omega - m\overline{v}}{\overline{u}} \tag{11}$$

$$k_4 = \frac{(\omega - m\overline{v})\,(\overline{a}\Psi - \overline{u})}{\overline{a}^2 - \overline{u}^2} \tag{12}$$

$$k_5 = -\frac{(\omega - m\overline{v})\,(\overline{a}\Psi + \overline{u})}{\overline{a}^2 - \overline{u}^2} \tag{13}$$

with speed of sound $a$ and

$$\Psi = \begin{cases} \sqrt{\Delta} & \text{if } \Delta > 0, \\ -\mathrm{i}\ \mathrm{sign}\,(\omega - m\overline{v})\sqrt{-\Delta} & \text{if } \Delta < 0 \end{cases} \tag{14}$$

and

$$\Delta = 1 - \frac{(\overline{a}^2 - \overline{u}^2)\,m^2}{(\omega - m\overline{v})^2}. \tag{15}$$

The wave numbers $k_{1,2,3}$ are real and the group velocity normal to the boundary $\frac{\partial \omega}{\partial k} = u$ is positive. Thus, the respective perturbations $r_{1,2,3}$ propagate convectively in flow direction. They are incoming waves at an inflow boundary and outgoing ones at an outflow. The calculation of $k_4$ and $k_5$ requires the distinction of two cases. If $\Delta > 0$ then $\Psi$ is real. For flows that are subsonic normal to the boundary it can be shown that one wave is incoming and one is outgoing. Taking the positive branch of the root yields the wave corresponding to $k_4$ also propagates in flow direction whereas the other one travels in the opposite direction. If $\Delta < 0$, $\Psi$ becomes complex. We choose the sign of $\Psi$ such that $\mathrm{Im}(k_4)$ is real and, according to equation (3), the corresponding wave propagates downstream, which is consistent with the case $\Delta > 0$. The wave associated with $k_5$ then again travels upstream. In the particular case of

$\Delta = 0$, acoustic resonance occurs, which involves additional challenges for the construction of boundary conditions [4, 14]. But this case is not considered in the present work.

For flows that are supersonic normal to the boundary, there is no upstream running wave. Yet, there are only very few axially supersonic turbomachinery applications and, secondly, supersonic inflow and outflow boundary conditions are rather straightforward and can be found in many textbooks on CFD (e.g. [15]). Hence, this paper does not consider boundary conditions for normally supersonic flows.

To write down the eigenvectors and formulate boundary conditions based upon them, it is convenient to define

$$\lambda = \frac{m}{\omega}. \tag{16}$$

The matrix of right eigenvectors $R = (r_1\ r_2\ r_3\ r_4\ r_5)$ is defined by:

$$R(\lambda) = \begin{pmatrix} -\overline{\varrho} & 0 & 0 & \frac{\overline{\varrho}(1-(1-\overline{v}\lambda)Ma_x\Psi)}{2(1-Ma_x)} & \frac{\overline{\varrho}(1+(1-\overline{v}\lambda)Ma_x\Psi)}{2(1+Ma_x)} \\ 0 & \overline{a}\,\overline{u}\lambda & 0 & \frac{\overline{a}(1-\overline{v}\lambda)(\Psi-Ma_x)}{2(1-Ma_x)} & \frac{-\overline{a}(1-\overline{v}\lambda)(\Psi+Ma_x)}{2(1+Ma_x)} \\ 0 & \overline{a}\,(1-\overline{v}\lambda) & 0 & \frac{\overline{a}^2\left(1-Ma_x^2\right)\lambda}{2(1-Ma_x)} & \frac{\overline{a}^2\left(1-Ma_x^2\right)\lambda}{2(1+Ma_x)} \\ 0 & 0 & \overline{a} & 0 & 0 \\ 0 & 0 & 0 & \frac{\overline{\varrho}\,\overline{a}^2(1-(1-\overline{v}\lambda)Ma_x\Psi)}{2(1-Ma_x)} & \frac{\overline{\varrho}\,\overline{a}^2(1+(1-\overline{v}\lambda)Ma_x\Psi)}{2(1+Ma_x)} \end{pmatrix} \tag{17}$$

with $Ma_x$ denoting the boundary normal Mach number. From this, the significance of each right eigenvalue becomes apparent. As $r_1$ only affects the density, it constitutes an entropy perturbation. The second and third eigenvectors represent vorticity disturbances in the blade-to-blade plane and in spanwise direction, respectively. Since $\frac{\omega - m\overline{v}}{\overline{u}}$ is a triple eigenvalue of the dispersion relation (6), the determination of $r_1$, $r_2$ and $r_3$ is not unique. However, choosing them this way yields a physically vivid set of eigenvectors and their required orthogonality is evident at once. The two remaining eigenvectors correspond to upstream and downstream running acoustic perturbations, i.e. isentropic, irrotational pressure waves.

The left eigenvector matrix can be derived likewise. Another possibility to obtain the left eigenvector matrix is to invert the right eigenvector matrix:

$$L = \begin{pmatrix} l_1 \\ l_2 \\ l_3 \\ l_4 \\ l_5 \end{pmatrix} = R^{-1} = \begin{pmatrix} \frac{-1}{\overline{\varrho}} & 0 & 0 & 0 & \frac{1}{\overline{\varrho}\,\overline{a}^2} \\ 0 & \frac{-\overline{u}\lambda}{\overline{a}} & \frac{1-\overline{v}\lambda}{\overline{a}} & 0 & \frac{-\lambda}{\overline{\varrho}\,\overline{a}} \\ 0 & 0 & 0 & \frac{1}{\overline{a}} & 0 \\ 0 & \frac{1-\overline{v}\lambda}{a} & \frac{\overline{u}\lambda}{\overline{a}} & 0 & \frac{(1-\overline{v}\lambda)\Psi}{\overline{\varrho}\,\overline{a}^2} \\ 0 & -\frac{1-\overline{v}\lambda}{a} & -\frac{\overline{u}\lambda}{\overline{a}} & 0 & \frac{(1-\overline{v}\lambda)\Psi}{\overline{\varrho}\,\overline{a}^2} \end{pmatrix} \tag{18}$$

Due to the fact that there is one outgoing wave at an inflow and four outgoing waves at an outflow, we need to extrapolate outgoing perturbations from the interior. To do so, we define characteristic variables $c = (c_1\ c_2\ c_3\ c_4\ c_5)^T$ such that these characteristics coincide with the weights $\alpha_i$ in equation (9) for plane waves running perpendicularly to the boundary. Note this is the case if $m = 0$ or equivalently $\lambda = 0$. Hence, the forward and backward transformations are given by

$$c = L_{1d}\, q \tag{19}$$

with

$$L_{1d} = L(0) = \begin{pmatrix} \frac{-1}{\overline{\varrho}} & 0 & 0 & 0 & \frac{1}{\overline{\varrho}\,\overline{a}^2} \\ 0 & 0 & \frac{1}{\overline{a}} & 0 & 0 \\ 0 & 0 & 0 & \frac{1}{\overline{a}} & 0 \\ 0 & \frac{1}{a} & 0 & 0 & \frac{1}{\overline{\varrho}\,\overline{a}^2} \\ 0 & -\frac{1}{a} & 0 & 0 & \frac{1}{\overline{\varrho}\,\overline{a}^2} \end{pmatrix} \tag{20}$$

and

$$q = R_{1d}\, c \tag{21}$$

with

$$R_{1d} = R(0) = \begin{pmatrix} -\overline{\varrho} & 0 & 0 & \frac{\overline{\varrho}}{2} & \frac{\overline{\varrho}}{2} \\ 0 & 0 & 0 & \frac{\overline{a}}{2} & -\frac{\overline{a}}{2} \\ 0 & \overline{a} & 0 & 0 & 0 \\ 0 & 0 & \overline{a} & 0 & 0 \\ 0 & 0 & 0 & \frac{\overline{\varrho}\,\overline{a}^2}{2} & \frac{\overline{\varrho}\,\overline{a}^2}{2} \end{pmatrix}. \tag{22}$$

## 2.2 Steady boundary conditions

The boundary condition generally consists of two steps, i.e. mean flow conditions and circumferential perturbations are treated separately. As changes in the mean flow represent plane waves at the boundary, we can directly express them by changes in the 1D characteristics. In the following, we write down inflow and outflow boundary conditions by means of characteristics in a compact form, so equations for in- and outflow boundaries are only given separately where necessary. For this purpose, we separate the left and right eigenvector matrices and their corresponding characteristics depending on the direction of propagation of their associated waves. In normally subsonic flows, the first four waves propagate downstream and the fifth one runs upstream. Accordingly, we write for an inflow

$$\left(\begin{array}{c} L^{in} \\ \hline L^{out} \end{array}\right) = \left(\begin{array}{c} l_1 \\ l_2 \\ l_3 \\ l_4 \\ \hline l_5 \end{array}\right) \tag{23}$$

$$\left(\begin{array}{c} c^{in} \\ \hline c^{out} \end{array}\right) = \left(\begin{array}{c} c_1 \\ c_2 \\ c_3 \\ c_4 \\ \hline c_5 \end{array}\right) \tag{24}$$

$$\left(R^{in}\middle|R^{out}\right) = \left(r_1\ r_2\ r_3\ r_4\middle|\, r_5\right) \tag{25}$$

and for an outflow

$$\begin{pmatrix} \\ L^{out} \\ \\ \hline L^{in} \end{pmatrix} = \begin{pmatrix} l_1 \\ l_2 \\ l_3 \\ l_4 \\ \hline l_5 \end{pmatrix} \tag{26}$$

$$\begin{pmatrix} \\ c^{out} \\ \\ \hline c^{in} \end{pmatrix} = \begin{pmatrix} c_1 \\ c_2 \\ c_3 \\ c_4 \\ \hline c_5 \end{pmatrix} \tag{27}$$

$$\left(R^{out}\middle|R^{in}\right) = \left(r_1\ r_2\ r_3\ r_4\middle|\ r_5\right). \tag{28}$$

To meet the boundary values specified by the user, we define a residual vector for both inflow and outflow boundaries

$$\mathfrak{R}_{bd} = \begin{cases} \begin{pmatrix} \overline{p}(\overline{s} - s_{bd}) \\ \overline{\varrho}\,\overline{a}\,(\overline{v} - \overline{u}\tan(\alpha_{circ,bd})) \\ \overline{\varrho}\,\overline{a}\,(\overline{w} - \overline{u}\tan(\alpha_{rad,bd})) \\ \overline{\varrho}(\overline{h_t} - h_{t,bd}) \end{pmatrix} & \text{for inflow boundaries} \\ \\ \left(\overline{p} - p_{bd}\right) & \text{for outflow boundaries} \end{cases} \tag{29}$$

Here, the subscript $bd$ denotes user specified boundary values. Since for turbomachinery flows, the user commonly specifies stagnation pressure and stagnation temperature at an inflow boundary, the associated specific entropy $s$ and specific stagnation enthalpy $h_t$ need to be calculated from the former. The angles $\alpha_{circ}$ and $\alpha_{rad}$ represent the angles between the velocity vector and the boundary normal in pitchwise and spanwise direction. Mixing planes can be covered by defining analogously

$$\mathfrak{R}_{bd} = L^{in}_{1d}\,\delta\overline{q}_{mp} \tag{30}$$

with $\delta\overline{q}_{mp}$ being the difference between the flow states at each side of the mixing plane in the same frame of reference.

To meet the boundary values specified by the user or mixing plane, the required change of characteristics is obtained via a Newton-Raphson step:

$$\mathfrak{R}_{bd} + \frac{\partial\mathfrak{R}}{\partial q}\frac{\partial q}{\partial c^{in}}\delta\overline{c^{in}} = 0 \tag{31}$$

Note that $\frac{\partial q}{\partial c^{in}}$ is the backward transformation of the incoming characteristics, $R^{in}_{1d}$. The derivation of the residual Jacobian $\frac{\partial\mathfrak{R}}{\partial q}$ can be found in [10]. For the adaption of Giles' original boundary condition to a cell-centred solver, where the boundary condition is applied between two pseudo-time updates, we also need to modify the update of the mean charactersistics at the faces due the pseudo-time change of the outgoing characteristics in the interior [16]. We define another residual

$$\mathfrak{R}_i = L^{out}_{1d}\,(\overline{q_f} - \overline{q_i}) \tag{32}$$

where subscripts $i$ and $f$ denote inner cell values and face values, respectively. Note that the inner values have already been updated by the pseudo-time solver whereas face values are still about to be updated by the boundary condition. Finally, the update of mean characteristics reads

$$\delta\overline{c} = -L_{1d}\left[R^{in}_{1d}\left(\frac{\partial\mathfrak{R}}{\partial q}R^{in}_{1d}\right)^{-1}\mathfrak{R}_{bd} + R^{out}_{1d}\mathfrak{R}_i\right] \tag{33}$$

To apply the actual non-reflecting boundary condition, we perform a Fourier decomposition of the disturbances about the mean flow along the boundary in the pitchwise direction. The spatial transformation for any quantity $\phi$ reads

$$\hat{\phi}_i = \frac{1}{P}\int_0^P \widetilde{\phi}\, e^{-\mathrm{i}m_i\, y}\, dy. \tag{34}$$

with wave numbers $m_i = \frac{2\pi i+\theta}{P} \neq 0$, pitch $P$, inter-blade phase angle $\theta$ and local deviation from the average state $\widetilde{\phi} = \phi - \overline{\phi}$. Note that $\theta$ vanishes in steady computations. Accordingly, the backward transformation is given by

$$\widetilde{\phi} = Re\left(\sum_{i=-\infty}^{\infty}\hat{\phi}_i\, e^{\mathrm{i}m_i\, y}\right). \tag{35}$$

In order to attain non-reflecting properties at the boundary, equation (10) must be satisfied for every mode with $m_i \neq 0$ and $\omega = 0$. We can scale the second to fifth left eigenvectors by $\omega$ and then set $\omega$ to zero. Consequently, the left eigenvector matrix for steady boundary conditions reduces to

$$L_s = \begin{pmatrix} -\frac{1}{\overline{\varrho}} & 0 & 0 & 0 & \frac{1}{\overline{\varrho}\,\overline{a}^2} \\ 0 & -\frac{\overline{u}}{\overline{a}^2} & -\frac{\overline{v}}{\overline{a}^2} & 0 & \frac{-1}{\overline{\varrho}\,\overline{a}^2} \\ 0 & 0 & 0 & \frac{1}{\overline{a}} & 0 \\ 0 & -\frac{\overline{v}}{\overline{a}^2} & \frac{\overline{u}}{\overline{a}^2} & 0 & \frac{\beta}{\overline{\varrho}\,\overline{a}^3} \\ 0 & \frac{\overline{v}}{\overline{a}^2} & -\frac{\overline{u}}{\overline{a}^2} & 0 & \frac{\beta}{\overline{\varrho}\,\overline{a}^3} \end{pmatrix} \tag{36}$$

with

$$\beta = \begin{cases} \mathrm{i}\,\mathrm{sign}(m)\sqrt{\overline{a}^2 - (\overline{u}^2+\overline{v}^2)} & \text{for } \overline{u}^2+\overline{v}^2 < \overline{a}, \\ -\mathrm{sign}(\overline{v})\sqrt{(\overline{u}^2+\overline{v}^2) - \overline{a}} & \text{for } \overline{u}^2+\overline{v}^2 > \overline{a}. \end{cases} \tag{37}$$

We can express the actual boundary condition, equation (10), in terms of characteristics which is helpful to write the overall boundary update as a sum of mean characteristic changes and local changes. Note that the outgoing characteristics have to be extrapolated from the interior.

$$L^{in}_s\hat{q} = L^{in}_s\left(R^{in}_{1d}\,L^{in}_{1d}\,\hat{q}_f + R^{out}_{1d}\,L^{out}_{1d}\,\hat{q}_i\right) = L^{in}_s\left(R^{in}_{1d}\,\hat{c}^{in}_f + R^{out}_{1d}\,\hat{c}^{out}_i\right) = 0 \tag{38}$$

The above equation yields ideal values for the incoming characteristics as a function of the outgoing ones. To meet the ideal values, the required changes in the characteristic at an inflow boundary is given by

$$\begin{pmatrix}\delta\hat{c}_1\\ \delta\hat{c}_2\\ \delta\hat{c}_3\\ \delta\hat{c}_4\\ \delta\hat{c}_5\end{pmatrix} = \begin{pmatrix} -\hat{c}_{f,1} \\ -\frac{\beta+\overline{v}}{\overline{a}+\overline{u}}\hat{c}_{i,5} - \hat{c}_{i,2} \\ -\hat{c}_{f,3} \\ \left(\frac{\beta+\overline{v}}{\overline{a}+\overline{u}}\right)^2\hat{c}_{i,5} - \hat{c}_{f,4} \\ \hat{c}_{i,5} - \hat{c}_{f,5} \end{pmatrix}. \tag{39}$$

Accordingly, the outflow boundary condition reads

$$\begin{pmatrix} \delta\hat{c}_1 \\ \delta\hat{c}_2 \\ \delta\hat{c}_3 \\ \delta\hat{c}_4 \\ \delta\hat{c}_5 \end{pmatrix} = \begin{pmatrix} \hat{c}_{i,1} - \hat{c}_{f,1} \\ \hat{c}_{i,2} - \hat{c}_{f,2} \\ \hat{c}_{i,3} - \hat{c}_{f,3} \\ \hat{c}_{i,4} - \hat{c}_{f,4} \\ \frac{2\overline{u}}{\beta-\overline{v}}\hat{c}_{i,2} - \frac{\beta+\overline{v}}{\beta-\overline{v}}\hat{c}_{i,4} - \hat{c}_{f,5} \end{pmatrix}. \tag{40}$$

Subsequently, these characteristic changes can be transformed from the wavenumber domain back into the physical domain according to equation (35) yielding a local change of the characteristics $\delta\tilde{c}$.

For supersonic ($\overline{u}^2+\overline{v}^2 > \overline{a}^2$), but normally subsonic ($\overline{u} < \overline{a}$) flows, $\beta$ and $L_s$ are independent of $m$ according to equations (36) and (37). Hence, no Fourier transformation is required and equations (39) and (40) can be applied directly at each face substituting any $\hat{c}$ by $\widetilde{c}$. Note that the steady, supersonic boundary conditions become local boundary conditions in this case apart from their dependence on averaged quantities.

Prescribing no incoming perturbations means that entropy and enthalpy are uniform along the inflow boundary only within the linearised theory, but second-order perturbations may still occur. Thus, we replace the condition for $\delta\tilde{c}_1$ and $\delta\tilde{c}_4$ in the physical domain and instead enforce uniform entropy and enthalpy by locally driving the following residual

$$\begin{pmatrix} \widetilde{\mathfrak{R}_1} \\ \widetilde{\mathfrak{R}_2} \end{pmatrix} = \begin{pmatrix} \overline{p}\,\widetilde{s} \\ \overline{\varrho}\widetilde{h_t} \end{pmatrix} \tag{41}$$

to zero. This can be done by means of a Newton-Raphson step

$$\begin{pmatrix} \widetilde{\mathfrak{R}_1} \\ \widetilde{\mathfrak{R}_2} \end{pmatrix} + \begin{pmatrix} \frac{\gamma R}{\gamma-1}\overline{p} & 0 & 0 \\ \frac{\gamma}{\gamma-1}\overline{p} & \overline{\varrho}\,\overline{a}\,\overline{v} & \frac{\overline{\varrho}}{2}\left(\overline{a}^2 + \overline{a}\,\overline{u}\right) \end{pmatrix} \begin{pmatrix} \delta\tilde{c}_1 \\ \delta\tilde{c}_2 \\ \delta\tilde{c}_4 \end{pmatrix} = 0 \tag{42}$$

where $R$ denotes the specific gas constant. The resulting condition for the update of $\widetilde{c_1}$ and $\widetilde{c_4}$ reads

$$\begin{pmatrix} \delta\widetilde{c_1} \\ \delta\widetilde{c_4} \end{pmatrix} = \begin{pmatrix} -\frac{\gamma-1}{\gamma R}\widetilde{s} \\ \frac{-2}{\overline{a}(\overline{a}+\overline{u})}\left(\widetilde{h_t} + \frac{\widetilde{s}}{\gamma R}\overline{a}^2 + \overline{a}\,\overline{v}\,\delta\widetilde{c_2}\right) \end{pmatrix}. \tag{43}$$

We further have to determine the integral change of characteristics due to circumferential perturbations because the mean flow boundary conditions already ensure that averaged flow quantities match the boundary values specified by the user or the mixing plane. Accordingly, we have to subtract the integral change afterwards in order to guarantee the mean change of characteristics is not affected by the treatment of perturbations. For this purpose we introduce

$$\overline{\delta\widetilde{c}} = \frac{1}{P}\int_0^P \delta\widetilde{c}\,dy. \tag{44}$$

Finally, the overall update of a boundary face can be written as

$$\delta q = \left[\sigma R_{1d}^{in}\left(\delta\overline{c}^{in} + \delta\widetilde{c}^{in} - \overline{\delta\widetilde{c}^{in}}\right) + R_{1d}^{out}\left(\delta\overline{c}^{out} + \delta\widetilde{c}^{out} - \overline{\delta\widetilde{c}^{out}}\right)\right]. \tag{45}$$

The relaxation factor $\sigma$, which needs to be chosen suitably in the range of $0$ to $1$, is necessary to retain the well-posedness of the mathematical problem [7]. For the application in a cell-centred solver, the updated face values have to be extrapolated appropriately to the ghost cells.

### 2.3 Approximate unsteady boundary conditions

To overcome the disadvantage of the straightforward, exact unsteady NRBC being spatially and temporally non-local, Giles proposes an approximate, local unsteady boundary condition [7]. This approach has been introduced by Engquist and Majda for general wave equations [9], but Giles applied it to two-dimensional linearised Euler equations in general and turbomachinery flows in particular.

As in steady boundary conditions, the averaged flow field and perturbations are handled separately. The mean flow boundary condition is identical to the steady mean flow boundary condition except that averaged quantities in the residual (29) are additionally averaged in time rather than only circumferentially. Unsteady turbomachinery flows are (within the framework of RANS) considered to be periodic and, therefore, temporal averaging means averaging a quantity over one period in this context.

The actual approximate boundary condition, however, handles perturbations from the mean state. The condition for a (hypothetically) perfectly non-reflecting boundary treatment has been discussed in section 2.1. But the universal application of equations (10) and (18) requires the decomposition of the boundary flow field into the Fourier domain. To avoid this costly transformation, the central concept is to express the exact unsteady boundary condition by use of a Taylor series expansion about the one-dimensional characteristic boundary condition. Recall from equation (16) that $\lambda \rightarrow 0$ and from equations (15) and (14) that $\Psi \rightarrow 1$ in the one-dimensional case due to vanishing circumferential wave numbers $m$. Then, the second order approximation of the left eigenvector matrix $L$ reads

$$L_a = L|_{\lambda=0} + \lambda \left.\frac{\partial L}{\partial \lambda}\right|_{\lambda=0} = L_{1d} + \frac{m}{\omega} \left.\frac{\partial L}{\partial \lambda}\right|_{\lambda=0}. \tag{46}$$

Now the boundary condition $L_a^{in}\,\widetilde{q} = 0$ can be rearranged starting with multiplying by $\omega$. Comparing equations (1) and (4), we can infer that we can replace $\omega$ by $\mathrm{i}\frac{\partial}{\partial t}$ and $m$ by $-\mathrm{i}\frac{\partial}{\partial y}$ yielding

$$L_{1d}^{in}\frac{\partial \widetilde{q}}{\partial t} - \left.\frac{\partial L^{in}}{\partial \lambda}\right|_{\lambda=0} \frac{\partial \widetilde{q}}{\partial y} = 0. \tag{47}$$

Giles' shows his original formulation may become ill-posed at inflows [7]. To face this ill-posedness, he proposes a modification by giving up the perfect orthogonality of $l_4$ and $r_5$ and thereby the condition for perfect non-reflecting behaviour. A multiple of $(\lambda\, l_{2,1d})$ is added to $l_{a,4}$ such that $l_{a,4}\, r_5$ is minimized under the constraint of the inflow boundary condition being well-posed. Expressing $\widetilde{q}$ in terms of characteristics, we can again extrapolate the outgoing characteristic $\widetilde{c}_5$ from the interior and obtain the following inflow boundary condition

$$\frac{\partial}{\partial t}\begin{pmatrix}\widetilde{c}_1\\ \widetilde{c}_2\\ \widetilde{c}_4\end{pmatrix} + \begin{pmatrix}\overline{v} & 0 & 0\\ 0 & \overline{v} & \frac{1}{2}(\overline{a}+u)\\ 0 & \frac{1}{2}(\overline{a}-\overline{u}) & \overline{v}\end{pmatrix}\frac{\partial}{\partial y}\begin{pmatrix}\widetilde{c}_1\\ \widetilde{c}_2\\ \widetilde{c}_4\end{pmatrix} + \begin{pmatrix}0\\ \frac{1}{2}(\overline{a}-\overline{u})\\ 0\end{pmatrix}\frac{\partial \widetilde{c}_5}{\partial y} = 0. \tag{48}$$

The outflow boundary condition is already well-posed in its original formulation and, thus, remains unchanged. It reads

$$\frac{\partial \widetilde{c}_5}{\partial t} + \overline{v}\frac{\partial \widetilde{c}_5}{\partial t} + \begin{pmatrix}0 & \frac{1}{2}(\overline{a}+\overline{u}) & 0\end{pmatrix}\frac{\partial}{\partial y}\begin{pmatrix}\widetilde{c}_1\\ \widetilde{c}_2\\ \widetilde{c}_4\end{pmatrix} = 0. \tag{49}$$

As the characteristic $c_3$, representing vorticity perturbations in spanwise direction, is decoupled in this quasi-three-dimensional approach, this characteristic is treated as a convective perturbation and, hence, extrapolated appropriately.

The appropriate numerical method to solve these differential equations at the boundaries depends on the solution methods for the flow equations in the interior. The solution algorithm applied in TRACE is presented in [5]. The primitive variables at the boundary and in the ghost cells are reconstructed from the change of characteristics in the same manner as in the steady boundary conditions.

Due to the chosen approach, to express the left eigenvector matrix by a Taylor series expansion of order two in $\lambda$, this boundary is only perfectly non-reflecting for planar waves impinging normally upon the boundary. In general, the boundary conditions become more reflecting with increasing $\lambda$. Accordingly, flows with large circumferential wave numbers and flows that are dominated by low frequency perturbations can induce spurious reflections at the boundary. The non-reflecting properties of the inflow boundary condition are further diminished by the modification to gain well-posedness. Details on reflections coefficients can be found in [7] and applications to two-dimensional pressure-waves in uniform mean flow assessing the reflection properties are presented in [17].

A first order approximation of these boundary conditions is also implemented in TRACE. In the application section of this paper, both boundary conditions are applied and compared to the exact approach. Note that the first order approximation can also be regarded as a characteristic, one-dimensional boundary condition.

### 2.4 Exact NRBC

It can be difficult to distinguish between the impact of approximate, unsteady boundary conditions and actual unsteady effects when comparing unsteady and steady flow simulations. The authors rank direct comparability of steady and unsteady computations as highly desirable in order to asses unsteady flow phenomena in turbomachinery design and research. Therefore, we do not consider Fourier transforms in time and space to be necessarily circumvented due to their computational effort. The fundamental concept of the exact boundary conditions is applying condition (10) to any incoming mode of the spatially and temporally decomposed boundary flow field. For this purpose, we first determine the temporal Fourier decomposition at the boundary according to the approach He proposed in the context of his phase lag method [18]. For the implementation in TRACE, the reader is referred to [19]. The choice of considered harmonics is analogous to the phase lag set of harmonics. From here on, we distinguish temporally Fourier transformed quantities, denoted by subscript $\omega$, and circumferentially Fourier transformed quantities, denoted by subscript $m$. For simplicity, this has been omitted up to this point. The temporal Fourier coefficients $\hat{q}_\omega$ are again expressed in terms of characteristic variables $\hat{c}_\omega = L_{1d}\hat{q}_\omega$. For each frequency in the Fourier domain, the flow can also be Fourier transformed along the boundary according to equation (34) and the respective outgoing characteristics are again extrapolated from the interior characteristics $\hat{c}^{out}_{(\omega,m),i}$ . The exact non-reflecting boundary condition for every mode, i.e. for every combination of $\omega$ and $m$, reads

$$L^{in}\hat{q}_{(\omega,m),f} = L^{in}\left(R^{in}_{1d}\,\hat{c}^{in}_{(\omega,m),target} + R^{out}_{1d}\,\hat{c}^{out}_{(\omega,m),i}\right) = 0. \tag{50}$$

$L$ no longer needs to be approximated because $\omega$ and $m$ are known in this context. The condition for updating the incoming modal characteristics is

$$\delta\hat{c}^{in}_{(\omega,m)} = \left[-\left(L^{in}R^{in}_{1d}\right)^{-1} L^{in}R^{out}_{1d}\,\hat{c}_{(\omega,m),i}\right] - \hat{c}^{in}_{(\omega,m),f}. \tag{51}$$

The outgoing characteristic is modified according to

$$\delta\hat{c}^{out}_{(\omega,m)} = \hat{c}^{out}_{(\omega,m),i} - \hat{c}^{out}_{(\omega,m),f} \tag{52}$$

The mean flow $\hat{q}_{0,0}$ is treated in the same manner as in the steady or approximate unsteady boundary condition according to equation (33).

Transforming $\delta\hat{c}_{(\omega,m)}$ back into the physical domain, we obtain face-wise, harmonic characteristics $\delta\hat{c}_{\omega}(y)$. The change of primitive variables at each face is relaxed again:

$$\delta\hat{q}_{\omega} = \sigma R_{1d}\delta\hat{c}_{\omega} \tag{53}$$

Subsequently, the boundary states can be extrapolated to the ghost cells in the frequency domain. Finally, the current ghost cell state is reconstructed by means of an approximate, inverse Fourier transform, again exploiting the phase lag functionality in TRACE [19].

Due to its universal approach, this boundary condition is suitable and consistent for both steady and unsteady simulations. Beyond, this approach is perfectly consistent with the non-reflecting boundary condition for frequency domain methods, presented by Frey [20, 21], which is rather favourable to compare unsteady time-domain computations and frequency domain computations. Chassaing and Gerolymos [17] demonstrate the advantageous reflection properties towards Giles' approximate boundary conditions for certain acoustic waves in uniform mean flow. Yet, they observe considerably slower convergence. This is considered by the authors of this paper to be due to the issue of temporal Fourier coefficients evolving rather slowly over possibly many periods, which is a known handicap of the phase lag approach.

## 3 APPLICATION

To validate our implementation of the exact boundary conditions and asses their non-reflecting properties, we show their application to two turbomachinery test cases. The behaviour of the exact NRBC is compared to steady NRBC, first and second order approximate NRBC and simple, one-dimensional, steady Riemann boundary conditions. For the description of Riemann boundary conditions, the reader is referred to [15].

When discussing boundary conditions for turbomachinery flows, the appropriate definition of a mean state is not trivial. This issue has been excluded from the theory section to stick to the actual subject of non-reflecting boundary conditions. In the following applications, however, all mean flow states are obtained by flux averaging [10] along the pitch and additionally in time for unsteady flows.

All computations are performed on structured grids using DLR's finite-volume 3D RANS solver TRACE [22, 23] applying Roe's upwind scheme [24] extended to second order accuracy through van Leer's MUSCL extrapolation [25] and an appropriate limiter function for convective fluxes. Viscous fluxes are computed based on gradients obtained by a central finite difference scheme in combination with Wilcox's linear eddy viscosity turbulence model [26]. For steady simulations a first order implicit pseudo-time marching technique is employed. The same pseudo-time method is used for subiterations of single time steps in unsteady computations.

### 3.1 VKI LS89

The first test case is a two-dimensional, linear turbine cascade designed and investigated at the von Karman Institute for Fluid Dynamics. The airfoil is typical of high pressure turbine nozzle guide vanes. A detailed description can be found in [27].

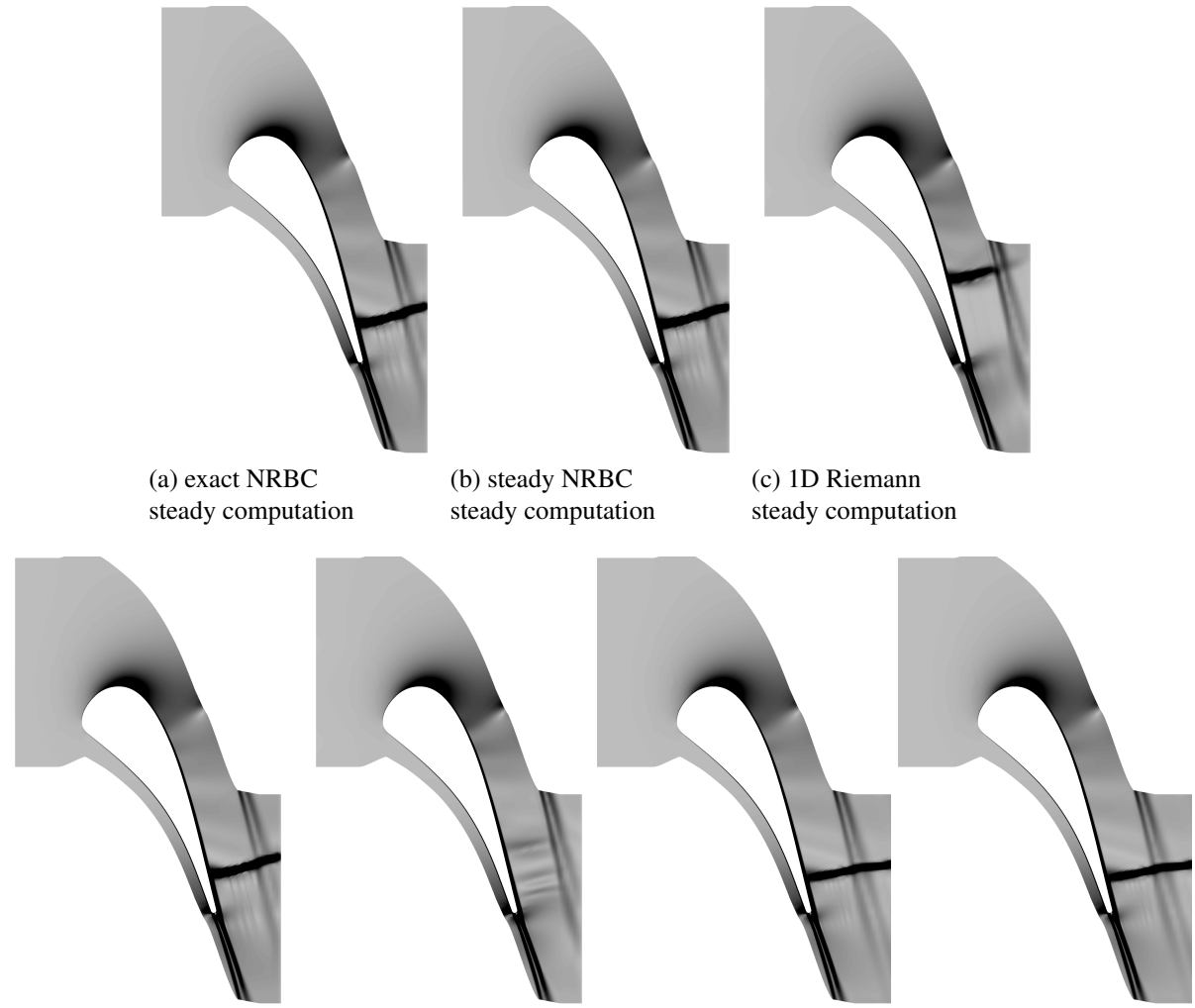

(a) exact NRBC steady computation

(b) steady NRBC steady computation

(c) 1D Riemann steady computation

(d) exact NRBC unsteady computation

(e) 2nd order approx. BC unsteady computation

(f) exact NRBC steady computation long domain

(g) steady NRBC steady computation long domain

Figure 1: Pseudo-Schlieren images obtained by plotting density gradient magnitude (black corresponds to large gradients)

All calculations are carried out for a supercritical operating point with 415 K stagnation temperature and 147500 Pa stagnation pressure at the inlet and 78000 Pa static pressure at the outlet. The inflow is purely axial. Steady computations are conducted applying one-dimensional Riemann boundary conditions, steady NRBC and exact NRBC.

Unsteady computations apply the second order approximate boundary conditions and the exact NRBC. The base frequency is set to 6100 Hz. The underlying assumption is that a downstream rotor blade with the same pitch faces purely axial flow in its relative frame of reference at this blade passing frequency. Therefore, this frequency is estimated to have a realistic order of magnitude for turbomachinery flows. One period is resolved by 64 time steps using a second order Euler backward scheme. For every physical time step, 25 pseudo-time iterations are performed. Though we perform unsteady computations, both solutions converge to a steady state.

Inlet and outlet planes are located at 50 % axial chord length away from the leading and

training edge. The computational grid comprises 21016 cells. Furthermore, we conduct steady computations with axial spacing between boundaries and the blade of 300 % axial chord length applying steady and exact NRBC to produce reference results. The extended grid comprises 36668 cells.

In figure 1, the magnitude of the density gradients is plotted for all computations in order to mimic the Schlieren flow visualization technique. The flow around the airfoil is supercritical, characterised by a shock close to suction side trailing edge impinging upon the exit boundary of the short computational domain. The flow field predicted employing the steady (Fig. 1b) and exact NRBC (Fig. 1a) in steady computations as well as the exact NRBC in an unsteady computation (Fig. 1d) agree qualitatively with the reference results obtained from steady computations in the long domain applying both steady (Fig. 1g) and exact NRBC (Fig. 1f). The shock position, in particular, is well captured.

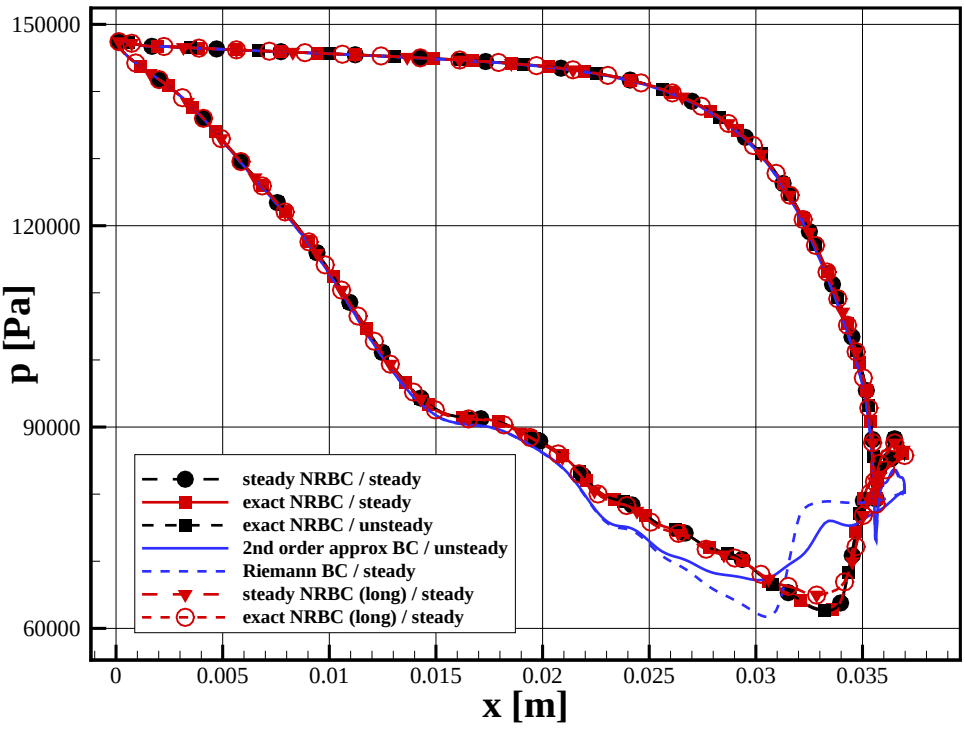


Figure 2: Blade pressure distribution

However, the solution obtained by Riemann boundary conditions (Fig. 1c) shifts the shock slightly upstream and diminishes its intensity. In the flow field resulting from the unsteady computation employing the second order approximate boundary condition (Fig. 1e), a distinct shock is not visible. This behaviour becomes more apparent in figure 2. Blade pressure distributions of all simulations are compared. The figure shows that the approximate boundary condition "smears out" the shock leading to a different suction side pressure distribution and, thus, aerodynamical load. Similarly, the Riemann boundary condition leads to a comparable error in the pressure distribution. The shift and weakening of the shock is evident here as well. Accordingly, an accurate prediction of integral forces, flow turning, performance and losses cannot be expected for this type of flow from the approximate boundary condition and the Riemann boundary condition.

The pressure distributions of all other computations coincide almost perfectly. Yet, in the very vicinity of the shock, all short domain computations deviate slightly from the reference results of the long domain. But among themselves, the exact and steady NRBC short domain results agree very well.

### 3.2 Transonic compressor rig

The second test case is a single-stage, transonic compressor rig of the Darmstadt University of Technology [28]. Steady and unsteady computations are performed for the aerodynamic design point. At a rotational speed of 20000 revolutions per minute the compressor achieves a stagnation pressure ratio of about 1.5 for a massflow of 16.3 kg/s. In order to conduct unsteady computations efficiently, the stator is scaled to 32 blades per row, which enables simulations having two stator blades and one rotor blade (16 blades per row) with equal pitch. The computational grid contains 254728 cells.

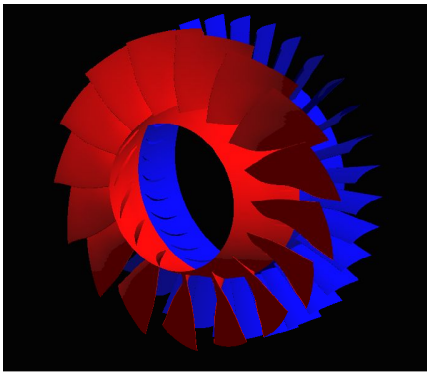

Figure 3: Computational model of the Darmstadt transonic compressor rig

Steady computations employ the mixing plane approach for blade row coupling [3], which is conservative due to its formulation based upon flux averaged quantities. Several computations are conducted applying one-dimensional Riemann boundary conditions, steady and exact NRBC. Unsteady computations utilize a conservative, non-matching interface [29] and a third order implicit Runge-Kutta time discretization scheme with 64 time steps per segment passing period. At each time step, 25 pseudo-time iterations are performed. First and second order approximate boundary conditions are applied as well as steady and exact NRBC.

Figure 4 shows the impact of boundary conditions on integral flow quantities in the compressor. The one-dimensional Riemann boundary conditions lead to an increase in the massflow of approximately 0.16 % compared to all other computations and 0.03 percentage points increase in isentropic efficiency towards steady computations employing steady and exact NRBC. This deviation is not huge, but significant in the context of turbomachinery performance analysis. All other solutions agree well regarding massflow and stagnation pressure ratio.

In particular, the steady and the exact NRBC predict abutting operation points and efficiencies. The shift in efficiency from steady to unsteady calculations can be explained from the inherently different mechanisms of loss production in steady and unsteady computations. Since any non-uniformity is mixed out in the mixing plane, this approach is known to overestimate losses in turbomachinery flows [30].

Considering the unsteady calculations, the influence of the chosen boundary condition on the operating point and performance is rather small. This might lead to the conclusion that steady boundary conditions can properly be applied in unsteady computations.

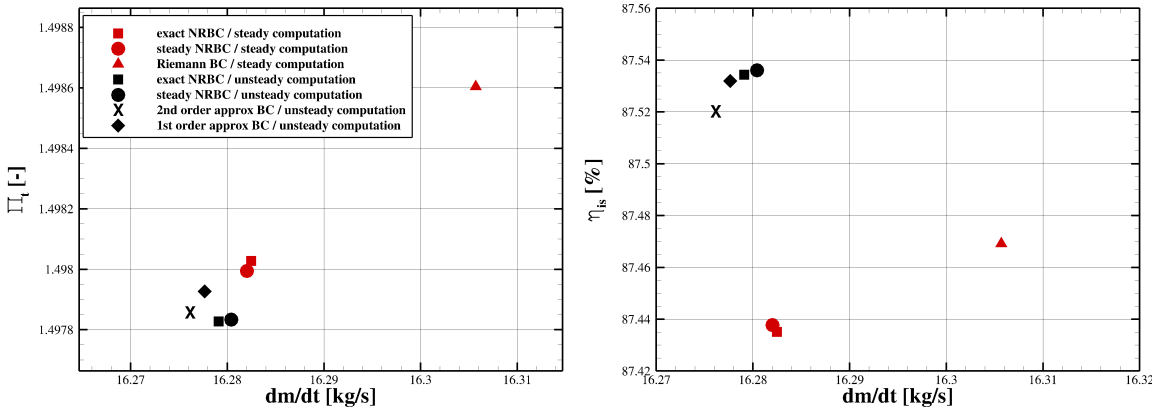


(a) Stagnation pressure ratio over massflow (b) Isentropic efficiency over massflow

Figure 4: Operating points for steady and unsteady computations employing different boundary conditions

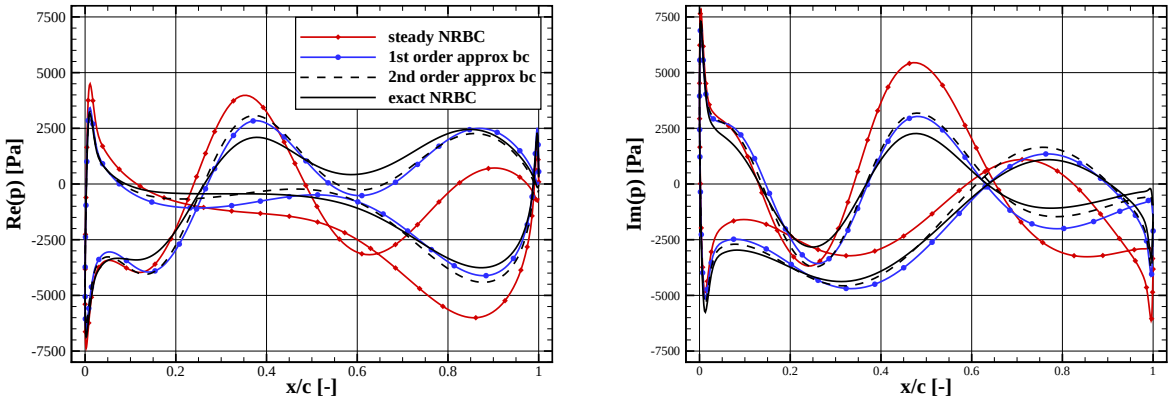


(a) Real part (b) Imaginery part

Figure 5: Unsteady blade pressure distribution along the 80 % relative mass flow streamsurface (complex Fourier coefficient of first harmonic)

However, even in the case of similar integral values, like massflow or efficiency, the flow field may still differ noticeably. The unsteady blade pressure distribution of the stator is depicted in figure 5. The plot shows the complex amplitude of pressure associated with the first harmonic (i.e. the segment passing frequency) along a stream surface that is defined such that 80 % of the overall massflow run through the passage below this stream surface. Due to artificial reflections arising when steady boundary conditions are applied in unsteady flows, the steady NRBC lead to a significantly different unsteady pressure distribution. The Exact NRBC and approximate NRBC yield comparable, but not perfectly matching unsteady pressure distributions.

Chassaing and Gerolymos demonstrate the good non-reflecting properties of the exact NRBC applied to unsteady flows with uniform underlying mean flow [17] whereas the derivation of the steady NRBC depends on the assumption of a steady flow field. Thus, it can be assumed that the exact NRBC provide a better prediction of the unsteady pressure field than the steady boundary conditions do. Since unsteady pressure fluctuations play a key role for aeroelastic and aeroacoustic phenomena, the inaccurate prediction of the unsteady pressure field can be

detrimental especially for these disciplines. Thus, the steady NRBC is not suitable for unsteady flows.

## 4 CONCLUSIONS

We have implemented an exact formulation of non-reflecting boundary conditions in TRACE, which is neither limited to steady flows nor suffers from the loss in accuracy raising from the approximation of the left eigenvectors. Thus, the presented exact NRBC represents a single method for both steady and unsteady turbomachinery flow simulations. Moreover, this method is consistent with the natural formulation of NRBC in frequency domain methods. However, the limitations arising from the linearisation of the quasi two-dimensional Euler equations still hold.

We have demonstrated the strong non-reflecting properties of the exact NRBC in two test cases. The steady flow in a two-dimensional supercritical, highly loaded turbine cascade is captured well. We observe good agreement with the non-reflecting steady NRBC as well as with reference solutions obtained on a larger domain. Moreover, the solution coincide when switching to unsteady simulations. This behaviour is advantageous compared to the combination of steady and approximate, unsteady boundary conditions since the flow field predicted employing the approximate unsteady NRBC varies significantly from the steady solution obtained employing steady NRBC. Note that no unsteadiness is observed in the unsteady solutions. So the change cannot be explained by unsteady effects.

The application to a transonic compressor stage showed that the exact method is capable to predict the operating point and performance in good agreement with the steady boundary condition. In contrast, less advanced one-dimensional Riemann boundary conditions diminish the solution quality in both test cases and are, therefore, considered inferior in turbomachinery flows.

We further demonstrated, that steady NRBC applied in unsteady computations do not necessarily predict significantly different integral quantities such as performance data or the operating point. However, in time resolving simulations, the steady NRBC lead to reflected waves that propagate through the domain and, possibly, pollute the simulation of unsteady flow phenomena.

In summary, the exact NRBC perform very satisfactory in both test cases. However, the lagged convergence properties due to the challenging determination of temporal Fourier coefficients may limit the range of practical applicability. Thus, investigations on this issue are needed to further improve convergence speed and robustness.

## ACKNOWLEGEMENT

Financial support by MTU Aero Engines (co-sponsorship of the first author) is gratefully acknowledged.

## REFERENCES

[1] J. D. Denton and W. N. Dawes, “Computational fluid dynamics for turbomachinery design,” *Proceedings of the Institution of Mechanical Engineers, Part C: Journal of Mechanical Engineering Science*, vol. 213, no. 2, pp. 107–124, 1998.

[2] W. Dawes, "Turbomachinery computational fluid dynamics: asymptotes and paradigm shifts," *Philosophical Transactions of the Royal Society of London A: Mathematical, Physical and Engineering Sciences*, vol. 365, no. 1859, pp. 2553–2585, 2007.

[3] J. Denton and U. Singh, "Time marching methods for turbomachinery flow calculations," VKI Lecture Series 1979-7, von Karman Institute., 1979.

[4] H.-P. Kersken, G. Ashcroft, C. Frey, N. Wolfrum, and D. Korte, "Nonreflecting boundary conditions for aeroelastic analysis in time and frequency domain 3D RANS solvers," in *Proceedings of ASME Turbo Expo 2014*, 2014.

[5] G. Ashcroft and J. Schulz, "Numerical modelling of wake-jet interaction with application to active noise control in turbomachinery," in *Proceedings of Aeroacoustics Conferences*, American Institute of Aeronautics and Astronautics, 2004.

[6] R. L. Higdon, "Initial-boundary value problems for linear hyperbolic systems," *SIAM Rev.*, vol. 28, pp. 177–217, June 1986.

[7] M. B. Giles, "Non-reflecting boundary conditions for the Euler equations," tech. rep., MIT Dept. of Aero. and Astr., 1988. CFDL Report 88-1.

[8] M. B. Giles, "Nonreflecting boundary conditions for Euler calculations," *AIAA Journal*, vol. 28, no. 12, pp. 2050–2058, 1990.

[9] B. Engquist and A. Majda, "Absorbing boundary conditions for the numerical simulation of waves," *Math. Comp.*, vol. 31, pp. 629–651, May 1977.

[10] M. Giles, "UNSFLO: A numerical method for the calculation of unsteady flow in turbomachinery," tech. rep., Gas Turbine Laboratory Report GTL 205, MIT Dept. of Aero. and Astro., 1991.

[11] A. P. Saxer and M. B. Giles, "Quasi-three-dimensional nonreflecting boundary conditions for Euler equations calculations.," *Journal of Propulsion and Power*, vol. 9, no. 2, pp. 263–271, 1993.

[12] T. Hagstrom, *Computational Wave Propagation*, ch. On High-Order Radiation Boundary Conditions, pp. 1–21. New York, NY: Springer New York, 1997.

[13] S. Henninger, P. Jeschke, G. Ashcroft, and E. Kügeler, "Time-domain implementation of higher-order non-reflecting boundary conditions for turbomachinery applications," in *Proceedings of ASME Turbo Expo 2013*, 2015.

[14] C. Frey and H.-P. Kersken, "On the regularisation of non-reflecting boundary conditions near acoustic resonance," in *Accepted for: Proceedings of ECCOMAS Congress 2016*, 2016.

[15] C. B. Laney, *Computational gasdynamics*. Cambridge University Press, 1998.

[16] S. Robens, C. Frey, P. Jeschke, E. Kügeler, A. Bosco, and T. Breuer, "Adaption of Giles non-local non-reflecting boundary conditions for a cell-centered solver for turbomachinery applications," in *Proceedings of ASME Turbo Expo 2013*, 2013.

[17] J. Chassaing and G. Gerolymos, "Time-domain implementation of nonreflecting boundary-conditions for the nonlinear euler equations," *Applied Mathematical Modelling*, vol. 31, no. 10, pp. 2172 – 2188, 2007.

[18] L. He, "Method of simulating unsteady turbomachinery flows with multiple perturbations," *AIAA Journal*, vol. 30, pp. 2730–2735, Nov. 1992.

[19] R. Schnell and D. Nürnberger, "Investigation of the tonal acoustic field of a transonic fanstage by time-domain CFD-calculation with arbitrary blade counts," in *Proceedings of ASME Turbo Expo 2004*, 2004.

[20] C. Frey, G. Ashcroft, H.-P. Kersken, and C. Voigt, "A harmonic balance technique for multistage turbomachinery applications," in *Proceedings of ASME Turbo Expo 2014*, 2014.

[21] C. Frey, G. Ashcroft, and H.-P. Kersken, "Simulations of unsteady blade row interactions using linear and non-linear frequency domain methods," in *Proceedings of ASME Turbo Expo 2015*, 2015.

[22] K. Becker, K. Heitkamp, and E. Kügeler, "Recent progress in a hybrid-grid CFD solver for turbomachinery flows," in *Proceedings Fifth European Conference on Computational Fluid Dynamics ECCOMAS CFD 2010*, 2010.

[23] K. Becker and G. Ashcroft, "A comparative study of gradient reconstruction methods for unstructured meshes with application to turbomachinery flows," in *52nd AIAA Aerospace Sciences Meeting*, (National Harbor, MD, USA), Jan. 2014.

[24] P. L. Roe, "Approximate Riemann solvers, parameter vectors, and difference schemes," *Journal of Computational Physics*, vol. 43, no. 2, pp. 357–372, 1981.

[25] B. van Leer, "Towards the ultimate conservative difference scheme. V. a second-order sequel to Godunov's method," *Journal of Computational Physics*, vol. 32, no. 1, pp. 101–136, 1979.

[26] D. C. Wilcox, "Reassessment of the scale-determining equation for advanced turbulence models," *AIAA Journal*, vol. 26, pp. 1299–1310, Nov. 1988.

[27] T. Arts and M. L. De Rouvroit, "Aero-thermal performance of a two dimensional highly loaded transonic turbine nozzle guide vane: A test case for inviscid and viscous flow computations," in *Proceedings of ASME Turbo Expo 1990*, 1990.

[28] G. Schulze, C. Blaha, D. Hennecke, and J. Henne, "The performance of a new axial single stage transonic compressor," in *Proceedings of the 12th International Symposium on Air Breathing Engines (ISABE)*, 1995.

[29] H. Yang, D. Nürnberger, and H.-P. Kersken, "Towards excellence in turbomachinery computational fluid dynamics," *Journal of Turbomachinery*, vol. 2006, no. 128, pp. 390–402, 2006.

[30] G. Fritsch and M. B. Giles, "An asymptotic analysis of mixing loss," *Journal of turbomachinery*, vol. 117, p. 367, 1995.